Published in final edited form as:
J Biomech. 2010 May 7; 43(7): 1322–1329. doi:10.1016/j.jbiomech.2010.01.018.

Biomechanical remodeling of obstructed guinea pig jejunum

Jingbo Zhao[1], **Donghua Liao**[1], **Jian Yang**[1], and **Hans Gregersen**[1,2]

[1] Mech-Sense, Aalborg Hospital Science and Innovation Centre (AHSIC), 9000 Aalborg, Denmark

[2] La Jolla Bioengineering Institute, La Jolla, California, USA

Abstract

Data on morphological and biomechanical remodeling are needed to understand the mechanisms behind intestinal obstruction. The effect of partial obstruction on mechanical properties with reference to the zero-stress state and on the histomorphological properties of the guinea pig small intestine was determined in this study. Partial obstruction and sham operation were surgically created in mid-jejunum of guinea pigs. The animals survived 2, 4, 7, and 14 days respectively. The age-matched guinea pigs that were not operated served as normal controls. The segment proximal to the obstruction site was used for histological analysis, no-load state and zero-stress state data, and distension test. The segment for distension was immersed in an organ bath and inflated to 10 cmH_20. The outer diameter change during the inflation was monitored using a microscope with CCD camera. Circumferential stresses and strains were computed from the diameter, pressure and the zero-stress state data. The opening angle and absolute value of residual strain decreased ($P<0.01$ and $P<0.001$) whereas the wall thickness, wall cross-sectional area, and the wall stiffness increased after 7 days obstruction ($P<0.05$, $P<0.01$). Histologically, the muscle and submucosa layers, especially the circumferential muscle layer increased in thickness after obstruction. The opening angle and residual strain mainly depended on the thickness of the muscle layer whereas the wall stiffness mainly depended on the thickness of the submucosa layer. In conclusion, the histomorphological and biomechanical properties of small intestine (referenced for the first time to the zero-stress state) remodel proximal to the obstruction site in a time-dependent manner.

Keywords

Jejunum; Partial obstruction; Hypertrophy; Stress-strain; Residual strain

1. Introduction

Small intestinal obstruction is a common clinical problem and causes structural remodelling and motility disturbances (DiBaise and Quigley, 1998). Intestinal obstruction can be caused by congenital malformation (Hernanz-Schulman, 2003; Miyamoto et al., 2005; Park and Vaezi, 2005) or can be acquired (Hsieh et al., 2005; Zollinger, 1986).

Several animal experimental models have been developed for small intestinal obstruction. In chronic obstruction, the intestinal wall hypertrophies and luminal dilatation occurs proximal

Address correspondences to: Jingbo Zhao, M.D., Ph.D., Mech-Sense, Aalborg Hospital Science and Innovation Centre (AHSIC), Sdr. Skovvej 15, DK-9000 Aalborg, Denmark, Phone: +45 99326907., jzhao@hst.aau.dk.

to the obstruction site (Bertoni and Gabella, 2001; Chang et al., 2001). Mechanical remodeling seems to play a major role in the pathophysiological process. Mechanical properties are a major determinant of tissue behavior and are likely the single most important factor determining tissue growth and remodeling (Fung, 1993). A better understanding of how gastrointestinal tissue adapts to mechanical changes is needed (Gregersen, 2002). Biomechanical data should be referenced to the zero-stress state; such data have been obtained from the small intestine of maturing rats (Lu et al., 2005) and diabetic rats (Zhao et al., 2003a, 2003b, 2006). Similar data are not available for the partially obstructed intestine despite the comprehensive work by Gabella (1975), Schulze-Delrieu (1995) and Storkholm (1995, 1998, 2007). Since biomechanics deals with the relation between stress and strain, we consider the intestinal zero-stress state, residual strain and stress-strain relationship as the relevant remodelling parameters because they are measures of the non-uniformity of intestinal growth (Gregersen and Kassab, 1996; Gregersen, 2002).

The aim of this study was to study time-dependent biomechanical and histomorphometric changes of the partially obstructed small intestine in guinea pigs.

2. Materials and methods

2.1. Animals and groups

Male guinea pigs (600-800g) were divided into 4 obstruction and 4 sham-operated control groups living for 2, 4, 7 and 14 days. Ten age-matched guinea pigs without operation were used as normal controls. We have long-term experience with the operation and kept the mortality rate below 20%. The final number of animals was 6 in each operation group and 4 in each sham-operated group. The guinea pigs had access to water but were restricted from food intake from the last night before the operations and experiments. The animals were weighted daily. The protocol was approved by the Danish Committee for Animal Experimentation.

2.2. Creation of partial small intestine obstruction in guinea pig

The surgical procedure for partially obstructing the small intestine is well-established (see detail in Storkholm et al., 2007). Briefly, following anesthesia and abdominal incision a 3.5 mm-wide polyurethane band was passed through the mesenteric window and closed antimesenterically with a 6-0 silk suture at a circumference about one millimetre longer than the outer intestinal circumference. In the sham group the mesenteric incision was made and marked with a 6-0 silk suture but no band was placed. The abdominal wall was closed with 4.0 silk. The animals were evaluated and weighed daily after the operation. Animals in poor clinical condition were euthanized and excluded from the study.

2.3. In vitro intestinal preparation

When the scheduled time had arrived, the guinea pig was anesthetized with Hypnorm and Dormicum. The abdominal cavity was opened with careful dissection of the intestine. A 10 cm small intestinal segment proximal to the band was removed. After measuring the length, the segment was immediately put into the organ bath containing Krebs solution with a gas mixture of 95% O_2-5% CO_2 at 37 °C, pH 7.4. First we did motility experiments (to be reported in a subsequent paper). Then, the intestinal segment was immersed in physiological saline containing papaverine (0.8×10^{-4} mM) for 30 min. to abolish contractile activity. The passive biomechanical test was done in the same organ bath using modified Krebs solution without $CaCl_2$ and glucose but with EGTA (100mg/L) at room temperature.

2.4. The zero-stress state of the intestinal segment

Methods for the determination of the gastrointestinal zero-stress state have been previously described (Gregersen, 2002). Two short ring-shaped segments were cut from the proximal end of the intestinal segments and transferred to Krebs solution. This represented the no-load state and photograph was taken. Then, the ring was cut radially and opened up into a sector. Photographs were taken ~30 min after to allow viscoelastic creep to take place. This represented the zero-stress state.

2.5. Distension of the intestinal segment

After measuring the initial length, the proximal end of intestinal segment was tied on a cannula using silk threads and connected to a pump (Genie Programmable Syringe Pump, WPI) (figure 1). The distal end of the segment was tied and connected to manipulator for applying longitudinal stretch. A small pressure probe was inserted into the intestinal lumen for measuring the luminal pressure. Ramp distension was done up to 10.0 cmH_2O pressure using a constant volume infusion rate of 0.8ml/min at 0, 10% and 20% longitudinal stretch. Images of the segment were captured by a CCD camera (SONY CCD Camera, Japan) and recorded by an S-Video (Panasonic NV-HS900, Kadoma, Japan) through a stereo microscope (WPI PZMIV, Sarasota, USA) with 25 pcs/sec. Pressures were recorded simultaneously by the Openlab program (Ditens A/S, Denmark). The video was transferred into a computer using a video card. The image resolution was 14 pixels per millimetre.

2.6. Histological analysis of the small intestine

After the distension experiment, the segment was fixed in 10% buffered formalin over 24 hours. Five-micron sections were cut and stained with haematoxylin and eosin. The layer thickness was measured. Twelve determinations were made on each specimen and averaged.

2.7. Mechanical data analysis

The following morphometric data were measured from digitised images of the segments in the zero-stress and no-load states by using image analysis software (Sigmascan Pro 4.0): the circumferential length (C), the wall thickness (h), and the wall area (A) at no-load and zero-stress state, and the opening angle (α) at zero-stress state. Furthermore, the outer diameter (D) was measured from the images of the pressurised segments by using a self made subroutine. The subscripts i, o, n, z and p refer to the mucosal surface, serosal surface, no-load state, zero-stress state and pressurised condition. The opening angle α was defined as the angle subtended by two radii drawn from the midpoint of the inner wall to the inner tips of two ends of the specimen.

The measured data was used for computation of biomechanical parameters defined as:

Residual Green's strain at the mucosal surface:

$$E_i=\frac{(\frac{C_{i-n}}{C_{i-z}})^2-1}{2} \quad [1]$$

Residual Green's strain at the serosal surface:

$$E_o = \frac{\left(\frac{C_{o-n}}{C_{o-z}}\right)^2 - 1}{2} \quad [2]$$

The circumferential stress and strain of the intestinal segment in the pressurised state were determined under assumptions that the wall was homogenous and the intestinal shape was cylindrical. The longitudinal stretch ratio λ_φ, the luminal radius r_{i-p}, the outer radius r_{o-p}, the wall thickness h_p and the circumferential stretch ratio λ_θ were obtained same as our previous studies (Gregersen, 2002; Zhao et al., 2003a). The Kirchhoffs stress and Green's strain were computed using the equations:

Circumferential Kirchhoff's stress:

$$S_\theta = \frac{\Delta \mathrm{Pr}_{i-p}}{h_p \lambda_\theta^2} \quad [3]$$

Circumferential midwall Green's strain:

$$E_\theta = \frac{\lambda_\theta^2 - 1}{2} \quad [4]$$

ΔP is the transmural pressure.

The stress-strain curves were fitted to the exponential function (Gregersen, 2002):

$$S = (S^* + b)e^{a(E-E^*)} - b \quad [5]$$

where a and b are material constants and S^* and E^* are circumferential Kirchhoff stress and Green strain at a specific point.

2.8. Statistical analysis

Results are expressed as means±SD. The constants obtained from the non-linear stress-strain fitting were used for the statistical evaluation. One way ANOVA was used to detect the differences for different parameters in the groups (Sigmastat 2.0™; Jandel Scientific, Erkrath, Germany). Linear and multiple linear regression analyses were used to demonstrate possible association between the biomechanical parameters and layer thickness. The results were regarded as significant when $P<0.05$.

3. Results

3.1. General data

The changes in body weight during the experiment were normalized as the body weight in a given day divided by the body weight at the start of the experiment. The weight linearly increased for the normal guinea pigs. Both for obstruction and sham operated groups, the weight decreased after the operation and reached the lowest point at day 3 for the obstruction groups and day 2 for the sham operated groups (Fig. 2). The sham operated

group recovered weight after 11 days. The obstructed animals did not reach the initial weight level again.

All motor activity was invariably abolished after adding papaverin and no contractile activity was elicited during distension.

The intestinal segments from the 2 days and 4 days obstruction animals were clearly dilated. After seven days, the intestinal segments were also visibly hypertrophied (Fig. 3). No apparent changes were observed in the sham obstruction and normal groups. The peritoneal lining had no signs of inflammation or adhesions that could potentially influence the mechanical properties.

3.2. Morphometry data

The wall thickness (Fig. 4A) and wall area (Fig. 4B) of the intestinal segments at no-load state gradually increased after obstruction. Statistical significance was reached after 7 days obstruction ($P<0.001$). At no-load state, the outer circumferential length (Fig. 4C) was significantly longer after 7 days obstruction ($P<0.01$ and $P<0.001$), whereas the inner circumferential lengths (Fig. 4D) was significantly longer after 14 days obstruction compared to sham operation and normal groups ($P<0.05$). The wall thickness, area, inner and outer circumferential lengths did not differ between the normal and sham-operated groups ($P>0.05$).

3.3. Histological data

The villous height and crypt depth did not differ between the groups (Fig. 5 top, $P>0.05$). The submucosa and muscle layers increased in a time-dependent manner after obstruction, especially the circumferential muscle layer increased up to 300% (Fig. 5 bottom). Significant difference was found after 7 days obstruction for the submucosa layer ($P<0.05$ and 0.01) and after 4 days obstruction for the muscle layer ($P<0.01$ and 0.001) compared with the normal and sham-operated control groups.

Representative samples of the muscle layer and submucosa layer proliferation is shown in Fig. 6. The thickness of both the submucosa layer and muscle layer increased during the development of the obstruction. Submucosa layer thickening was observed after 7 days obstruction. The cell number in the muscle layer started to increase after 2 days obstruction. Significant thickening of the layer was observed after 4 days obstruction mainly due to the increased cell numbers (hyperplasia). After 7 and 14 days obstruction, hypertrophy was clearly observed in both muscle layers and mainly accounted for the obvious thickening of the muscle layer. The circumferential muscle layer increased much more than the longitudinal muscle layer.

3.4. Biomechanical data

In brief, the opening angles and absolute values of residual strains were smaller after obstruction when compared to those with the sham-operated and normal groups (Fig. 7). For the opening angle (Fig. 7A), significant differences were found after 4 days obstruction compared with the normal group ($P< 0.01$ and $P< 0.001$) and after 7 days obstruction compared with sham-operated group ($P< 0.01$ and $P < 0.001$). For the inner and outer residual strains (Fig. 7B), significant differences were found after 14 days obstruction ($P< 0.05$, $P<0.01$ and $P< 0.001$). The changes in opening angle and residual strain mainly depended on the thickness of the muscle layer (see Table 1).

Fig. 8 (top) shows the circumferential stress-strain curves at longitudinal stretch ratio 1.1 in the different groups. The same pattern was found at stretch ratio 1.0 and 1.2 (data not

shown). The stress-strain curves were shifted to the left after 7 days obstruction compared to those with normal and sham-operated control groups, demonstrating the wall became stiffer. Furthermore, increasing the longitudinal stretch ratio shifts the stress-strain curves to the left, indicating that the longitudinal stretch increases circumferential wall stiffness. Corresponding with the stress-strain curves, the constant **a** was bigger in the 7 days and 14 days obstruction groups compared to other groups ($P<0.05$ and 0.01). The changes of constant **a** mainly depended on the thickness of the submucosa layer (Fig. 8, bottom).

4. Discussion

Understanding the relationship between the histomorphological remodeling and biomechanical remodeling caused by obstruction can shed more light on the mechanism and severity of intestinal function disorders. The present study shows that obstruction causes dilation and wall thickening, especially thickening of the circular muscle layer. Furthermore, the opening angle and residual strain decreased and the intestinal wall became stiffer. The opening angle and residual strain mainly depended on the thickness of the muscle layer whereas the stiffening mainly depended on thickening of the submucosa layer.

4.1. Methodology Aspects

The partially obstructed intestinal model has been validated previously (Bertoni et al., 2004; Schulze-Delrieu et al., 1995; Storkholm et al., 2007). The size of the band relative to the circumference of the intestine is important for successful obstruction. If the band is too tight the animal dies within 48 hours, if it is too loose no changes will occur (Storkholm et al., 2007). Although the band does not compress the resting intestine, during bolus passage the band is expected to increase the resistance during the propagation of contractions and movement of contents.

The biomechanical remodelling of partially obstructed intestine has not been previously studied with referenced to the zero-stress state (Storkholm et al., 2007). The zero-stress state of an organ is the state at which the organ is stress-free. Knowing the zero-stress configuration is essential in mechanical analysis since it serves as the reference state for computing stress and strain under physiological or pathophysiological conditions.

The passive biomechanical properties of soft tissues obtained at room temperature do not differ from those obtained at 37 °C (Liu and Fung, 1992). Therefore, for convenience reason we choose room temperature.

4.2. The pathophysiology of muscle layer thickening due to obstruction

Longstanding partial intestinal obstruction results in structural changes with marked dilatation and proliferation of the intestinal wall layers (Bertoni and Gabella, 2001; Bertoni et al., 2004; Chen et al., 2008; Gabella, 1990; Geuna et al., 1998; Storkholm et al., 2007, 2008). The present study confirmed that the intestinal wall thickness, wall area and circumferences, especially the muscle layer thickness increased during obstruction. The muscle layer increased circumferentially more than longitudinally probably due to increased circumferential stress.

Both the number and the size of muscle cells increase due to chronic obstruction (Gabella, 1975). The enlargement of the muscle cells (hypertrophy) likely account for the majority of the increase in the muscle layer thickness (Gabella, 1979a). The hypertrophied muscle cells exhibit ultra-structural changes of sarcoplasmic reticulum, gap connections, cytoplasmic content and increased ratio of myofilament to intermediate filament (Gabella, 1979b, 1979c, 1979d). The relative decrease in myofilament content suggests a loss of contractile machinery. However, the total contractile activity (force) of muscle layer after partial

obstruction increases due to the hyperplasia and hypertrophy of smooth muscle cells (Storkholm et al., 2008). More recently, Chen and co-workers (2008) demonstrated that a dynamic response of small intestinal muscles to the obstruction involving switching between differentiated, proliferative, and hypertrophic phenotypes. The serum response factors, myocardin, Elk-1, and c-fos might play key roles in the phenotypic switching. Furthermore, the intestinal collagen also changes during obstruction (Storkholm et al., 2007, 2008). We found that the submucosa layer thickness increased after intestinal obstruction. The interaction between smooth muscle cells and extracellular matrix have been extensively studied in airways and blood vessels (Hultgårdh-Nilsson and Durbeej, 2007; Zhang and Gunst, 2008). It has been reported that the stiffness of collagen fibrils influence vascular smooth muscle cell phenotype (McDaniel et al., 2007). Similar studies should be done on the obstructed intestine.

4.3. Biomechanical remodelling and its significances in the partial obstructed intestine

The zero-stress state is sensitive to remodelling by disease, growth or degeneration (Gregersen, 2002). The change of the opening angle is a result of non-uniform tissue remodelling of the organ wall. The opening angle increases when the inner layers grow more than the outer layers or when the outer layers atrophy more than the inner layers (Fung, 1993). The residual strain is the tissue deformation due to the residual stress. If the opening angle changes due to the intestinal non-uniform remodelling, the residual strain will change as well. Morphological and biomechanical data referenced to the zero-stress state have been obtained from the small intestine of maturing rats (Lu et al., 2005), fasting rats (Dou et al., 2002), rats treated with EGF (Zhao et al., 2002), and diabetic rats (Zhao et al., 2003a). The present study for the first time present the opening and residual strain distribution in the intestinal wall after partial obstruction. The opening angle and the absolute value of residual strain decreased after intestinal obstruction in a time-dependent manner. Since the obstruction-induced changes in the intestine primarily are in the muscle layers, the outer wall grows more than the inner wall and the opening angle decreased. Correspondingly, the outer residual strain became less tensile whereas the inner residual strain became less compressive. Multiple linear regression analysis confirmed that the changes of opening angle and residual strain mainly depended on the thickness of the muscle layer. The wall structure or deformation changes due to the obstruction likely alter the relative zero setting and the biomechanical remodelling of the residual strain and residual stress distribution likely alter the zero-setting of the stress in the mechanosensitive afferents. Consequently, the perception and motility of the GI tract may change as well.

Changes in the stress-strain distribution mainly reflect the structural remodelling of the intestinal wall during obstruction. Storkholm (2007) demonstrated that obstruction induced intestinal stiffening. Our study referenced to the zero-stress state demonstrated that the circumferential stiffness of the intestinal wall increased after 7 days obstruction. Multiple linear regression analysis demonstrated that the stiffness constant **a** mainly depended on the thickness of the submucosa layer. The submucosa layer is rich in collagen. Therefore, remodelling of the submucosa layer with increased collagen content likely determines the intestinal wall stiffness since collagen in most tissues is the stress-bearing structure (Fung, 1993). Increasing the stiffness of obstructed intestine will change the biomechanical environment of the nerve ending and muscle cells, and their network during the contraction and propagation, then further affect the intestinal function.

In conclusion, partial obstruction of small intestine induced growth of the intestinal wall in a time-dependent manner. The changes of opening angle and residual strain mainly depend on the thickness of the muscle layer whereas the change of the circumferential wall stiffness mainly depends on the thickness of the submucosa layer.

Acknowledgments

The studies were supported by NIH grant 1RO1DK072616-01A2 and the Danish Research Council.

References

Bertoni S, Gabella G. Hypertrophy of mucosa and serosa in the obstructed intestine of rats. Journal of Anatomy 2001;199(Pt 6):725–734. [PubMed: 11787826]

Bertoni S, Gabella G, Ghizzardi P, Ballabeni V, Impicciatore M, Lagrasta C, Arcari ML, Barocelli E. Motor responses of rat hypertrophic intestine following chronic obstruction. Neurogastroenterology & Motility 2004;16(3):365–374. [PubMed: 15198659]

Chang IY, Glasgow NJ, Takayama I, Horiguchi K, Sanders KM, Ward SM. Loss of interstitial cells of Cajal and development of electrical dysfunction in murine small bowel obstruction. The Journal of Physiology 2001;536(Pt 2):555–568. [PubMed: 11600689]

Chen J, Chen H, Sanders KM, Perrino BA. Regulation of SRF/CArG-dependent gene transcription during chronic partial obstruction of murine small intestine. Neurogastroenterology & Motility 2008;20(7):829–842. [PubMed: 18557893]

DiBaise JK, Quigley EM. Tumor-related dysmotility: gastrointestinal dysmotility syndromes associated with tumors. Digestive Diseases and Sciences 1998;43(7):1369–1401. [PubMed: 9690371]

Dou Y, Gregersen S, Zhao J, Zhuang F, Gregersen H. Morphometric and biomechanical intestinal remodeling induced by fasting in rats. Digestive Diseases and Sciences 2002;47(5):1158–1168. [PubMed: 12018916]

Fung, YC. Biomechanics Properties of living tissues. Springer-Verlag; Berlin: 1993.

Gabella G. Hypertrophy of intestinal smooth muscle. Cell and Tissue Research 1975;163(2):199–214. [PubMed: 1182787]

Gabella G. Hypertrophic smooth muscle. I. Size and shape of cells, occurrence of mitoses. Cell and Tissue Research 1979a;201(1):63–78. [PubMed: 527016]

Gabella G. Hypertrophic smooth muscle. II. Sarcoplasmic reticulum, caveolae and mitochondria. Cell and Tissue Research 1979b;201(1):79–92. [PubMed: 527017]

Gabella G. Hypertrophic smooth muscle. III. Increase in number and size of gap junctions. Cell and Tissue Research 1979c;201(2):263–76. [PubMed: 509483]

Gabella G. Hypertrophic smooth muscle. IV. Myofilaments, intermediate filaments and some mechanical properties. Cell and Tissue Research 1979d;201(2):277–88. [PubMed: 574421]

Gabella G. Hypertrophy of visceral smooth muscle. Anatomy and embryology (Berl) 1990;182(5): 409–424.

Geuna S, Cardillo S, Giacobini-Robecchi MG. Smooth muscle cell hypertrophy and hyperplasia in the partially obstructed gut of the rat: a quantitative evaluation. ACTA ANATOMICA (BASEL) 1998;163(2):69–74.

Gregersen, H. Biomechanics of the gastrointestinal tract New perspectives in motility research and diagnostics. Springer-Verlag; London: 2002.

Gregersen H, Kassab G. Biomechanics of the gastrointestinal tract. Neurogastroenterology & Motility 1996;8(4):277–297. [PubMed: 8959733]

Hernanz-Schulman M. Infantile hypertrophic pyloric stenosis. Radiology 2003;227(2):319–331. [PubMed: 12637675]

Hsieh TK, Chen AC, Wu SF, Chen W. Postoperative intussusception in children with enterostomy. Acta Paediatrica Taiwanica 2005;46(3):166–169. [PubMed: 16231566]

Hultgårdh-Nilsson A, Durbeej M. Role of the extracellular matrix and its receptors in smooth muscle cell function: implications in vascular development and disease. Current Opinion in Lipidology 2007;18(5):540–545. [PubMed: 17885425]

Liu SQ, Fung YC. Influence of STZ-induced diabetes on zero-stress states of rat pulmonary and systemic arteries. Diabetes 1992;41(2):136–146. [PubMed: 1733801]

Lu X, Zhao J, Gregersen H. Small intestinal morphometric and biomechanical changes during physiological growth in rats. Journal of Biomechanics 2005;38(3):417–426. [PubMed: 15652539]

McDaniel DP, Shaw GA, Elliott JT, Bhadriraju K, Meuse C, Chung KH, Plant AL. The stiffness of collagen fibrils influences vascular smooth muscle cell phenotype. Biophysical Journal 2007;92(5):1759–1769. [PubMed: 17158565]

Miyamoto M, Egami K, Maeda S, Ohkawa K, Tanaka N, Uchida E, Tajiri T. Hirschsprung's disease in adults: report of a case and review of the literature. Journal of Nippon Medical School 2005;72(2): 113–120. [PubMed: 15940019]

Park W, Vaezi MF. Etiology and pathogenesis of achalasia: the current understanding. The American Journal of Gastroenterology 2005;100(6):1404–1414. [PubMed: 15929777]

Schulze-Delrieu K, Brown B, Herman B, Brown CK, Lawrence D, Shirazi S, Palmieri T, Raab J. Preservation of peristaltic reflex in hypertrophied ileum of guinea pig. American Journal of Physiology, Gastrointestinal and Liver Physiology 1995;269(1 Pt 1):G49–G59.

Storkholm JH, Villadsen GE, Jensen SL, Gregersen H. Passive elastic wall properties in isolated guinea pig small intestine. Digestive Diseases and Sciences 1995;40(5):976–982. [PubMed: 7729287]

Storkholm JH, Villadsen GE, Jensen SL, Gregersen H. Mechanical properties and collagen content differ between isolated guinea pig duodenum, jejunum, and distal ileum. Digestive Diseases and Sciences 1998;43(9):2034–2041. [PubMed: 9753270]

Storkholm JH, Zhao J, Villadsen GE, Hager H, Jensen SL, Gregersen H. Biomechanical remodeling of the chronically obstructed guinea pig small intestine. Digestive Diseases and Sciences 2007;52(2): 336–346. [PubMed: 17219069]

Storkholm JH, Zhao J, Villadsen GE, Gregersen H. Spontaneous and bolus-induced motility in the chronically obstructed guinea-pig small intestine in vitro. Digestive Diseases and Sciences 2008;53(2):413–420. [PubMed: 17562174]

Zhang W, Gunst SJ. Interactions of airway smooth muscle cells with their tissue matrix: implications for contraction. Proceedings of the American Thoracic Society 2008;5(1):32–39. [PubMed: 18094082]

Zhao J, Yang J, Vinter-Jensen L, Zhuang F, Gregersen H. The morphometry and biomechanical properties of the rat small intestine after systemic treatment with epidermal growth factor. Biorheology 2002;39(6):719–733. [PubMed: 12454438]

Zhao J, Yang J, Gregersen H. Biomechanical and morphometric intestinal remodelling during experimental diabetes in rats. Diabetologia 2003a;46(12):1688–1697. [PubMed: 14593459]

Zhao J, Liao D, Yang J, Gregersen H. Viscoelastic behavior of small intestine in streptozotocin-induced diabetic rats. Digestive Diseases and Sciences 2003b;48(12):2271–2217. [PubMed: 14714612]

Zhao J, Frøkjaer JB, Drewes AM, Ejskjaer N. Upper gastrointestinal sensory-motor dysfunction in diabetes mellitus. World Journal of Gastroenterology 2006;12(18):2846–2857. [PubMed: 16718808]

Zollinger RM Jr. Primary neoplasms of the small intestine. American Journal of Surgery 1986;151(6): 654–658. [PubMed: 2424326]

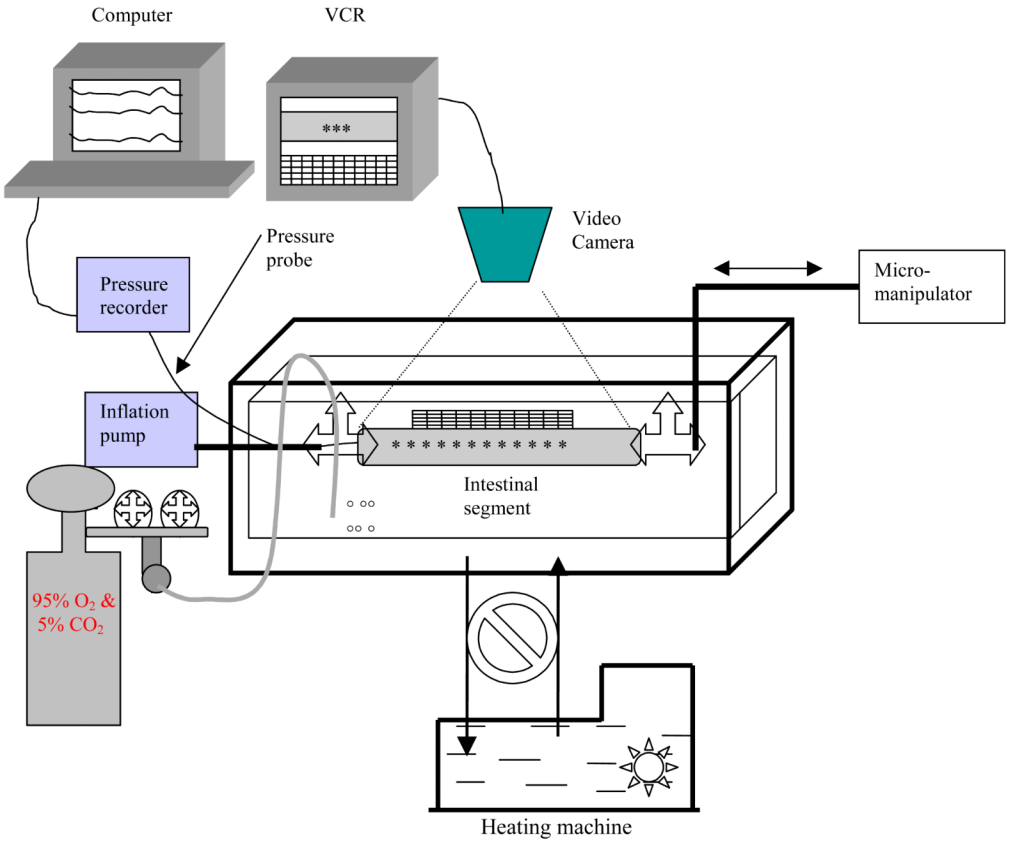

Figure 1.

Set-up of experiment.

The organ bath is composed of an inside small chamber and an outside chamber. The Krebs solution contained in the small chamber was maintained constant at 37 °C by circulating water in the big chamber using a heating machine. The intestinal segment was placed in the small chamber containing Krebs solution. The volume was applied by a pump and the stretch ratio regulated by a micromanipulator. The pressure probe was used to measure the pressures. The diameter changes of the intestinal segments were videotaped through a stereomicroscope.

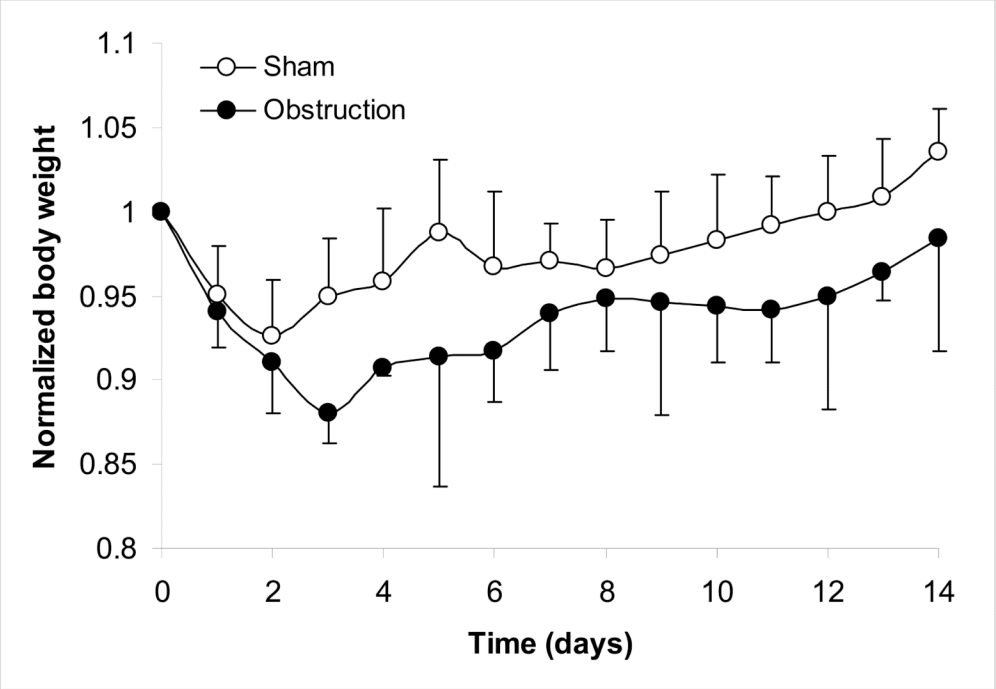

Figure 2.
The body weight decreased after the operation and reached the lowest point at 3 days for obstruction and 2 days for sham operation.

Figure 3.
Mid-jejunal segments obtained from 14 days sham operation (top) and from 14 days obstruction (bottom) guinea pigs. The arrows show the marker for sham operation and ring for obstruction. The intestinal wall was visibly hypertrophied and dilated proximal to the obstruction, whereas no apparent change was observed in the sham-operated animal.

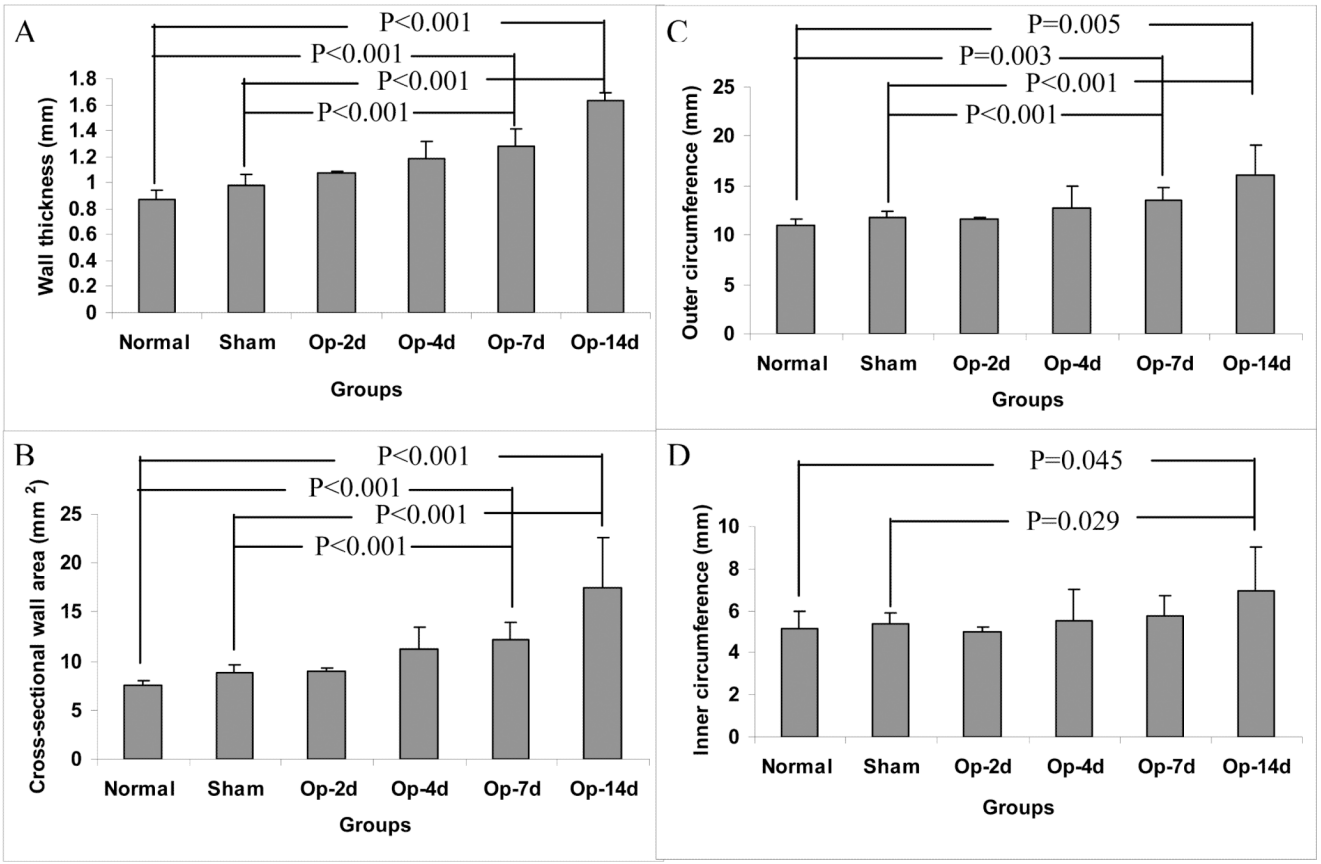

Figure 4.

Morphometry data: Compared with the normal and sham operated groups, the wall thickness (Fig. 4A), wall area (Fig. 4B), inner circumference (Fig. 4C) and outer circumference (Fig. 4D) of the intestinal segments at no-load state gradually increased after obstruction. The morphometric data did not differ between normal and sham operation groups.

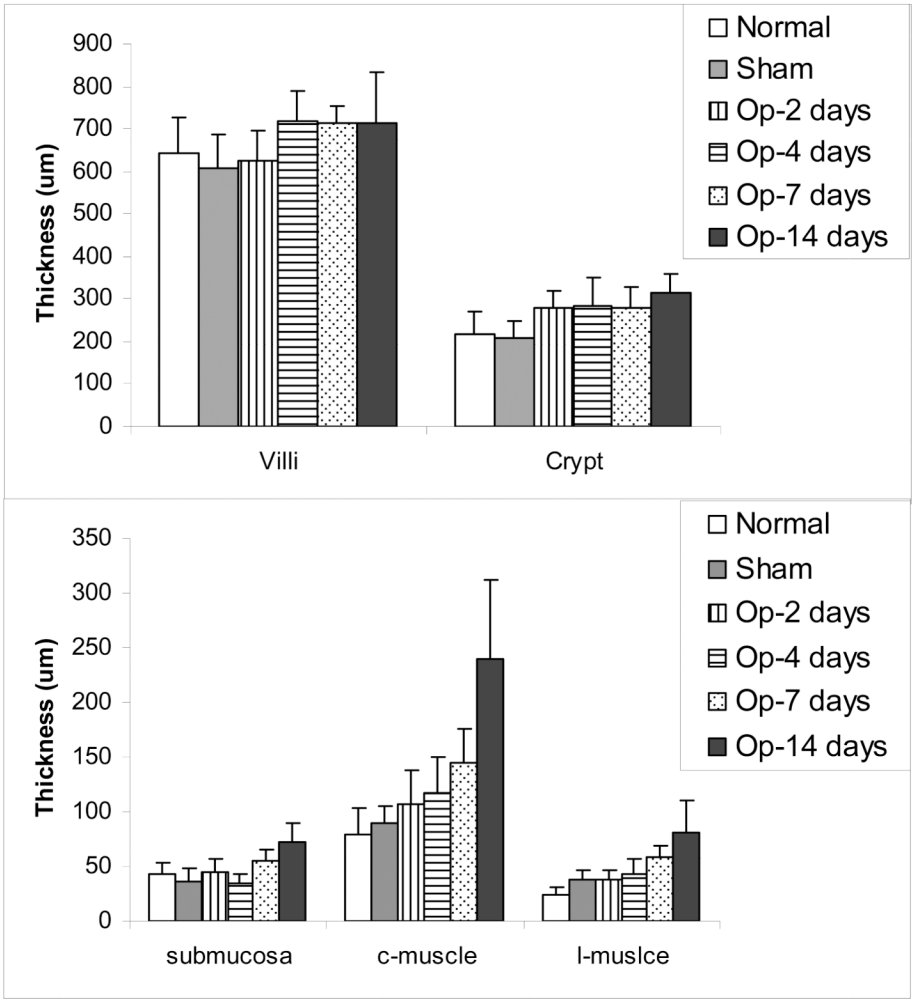

Figure 5.
The layer thickness: The villous height and crypt depth (mucosa thickness) did not differ between the groups (Fig. 5 top), whereas the submucosa and muscle layers increased in a time-dependent manner after obstruction, especially the circumferential muscle layer increased (Fig. 5 bottom).

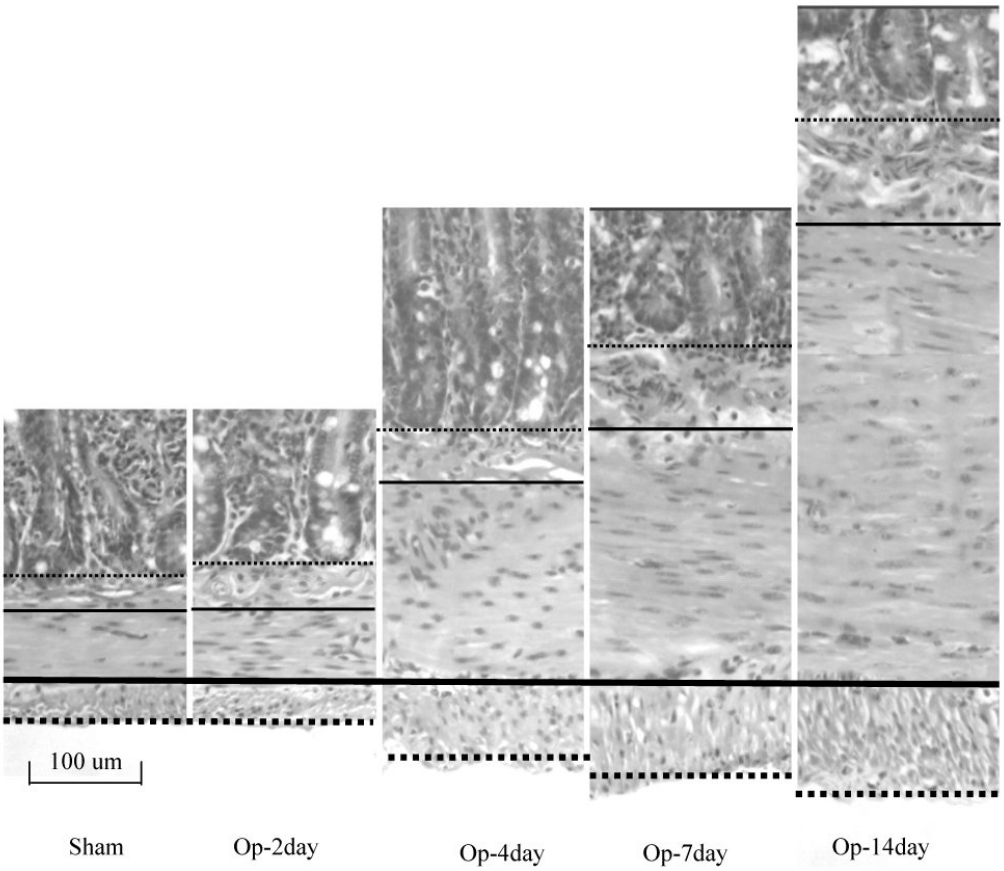

Figure 6.

The typical pattern of the muscle layer proliferation and submucosa thickning. The thick dense-line, the thin dense-line, the thick dot-line and thin dot-line indicated the interface of two muscle layers, outer bordering of longitudinal muscle layer, the interface between muscle layer and submocosa layer, and the interface between submucosa layer and mucosa layer. The submucosa and muscle layers increased the thickness after the obstruction, the circumferential muscle layer increased much more than the longitudinal muscle layer.

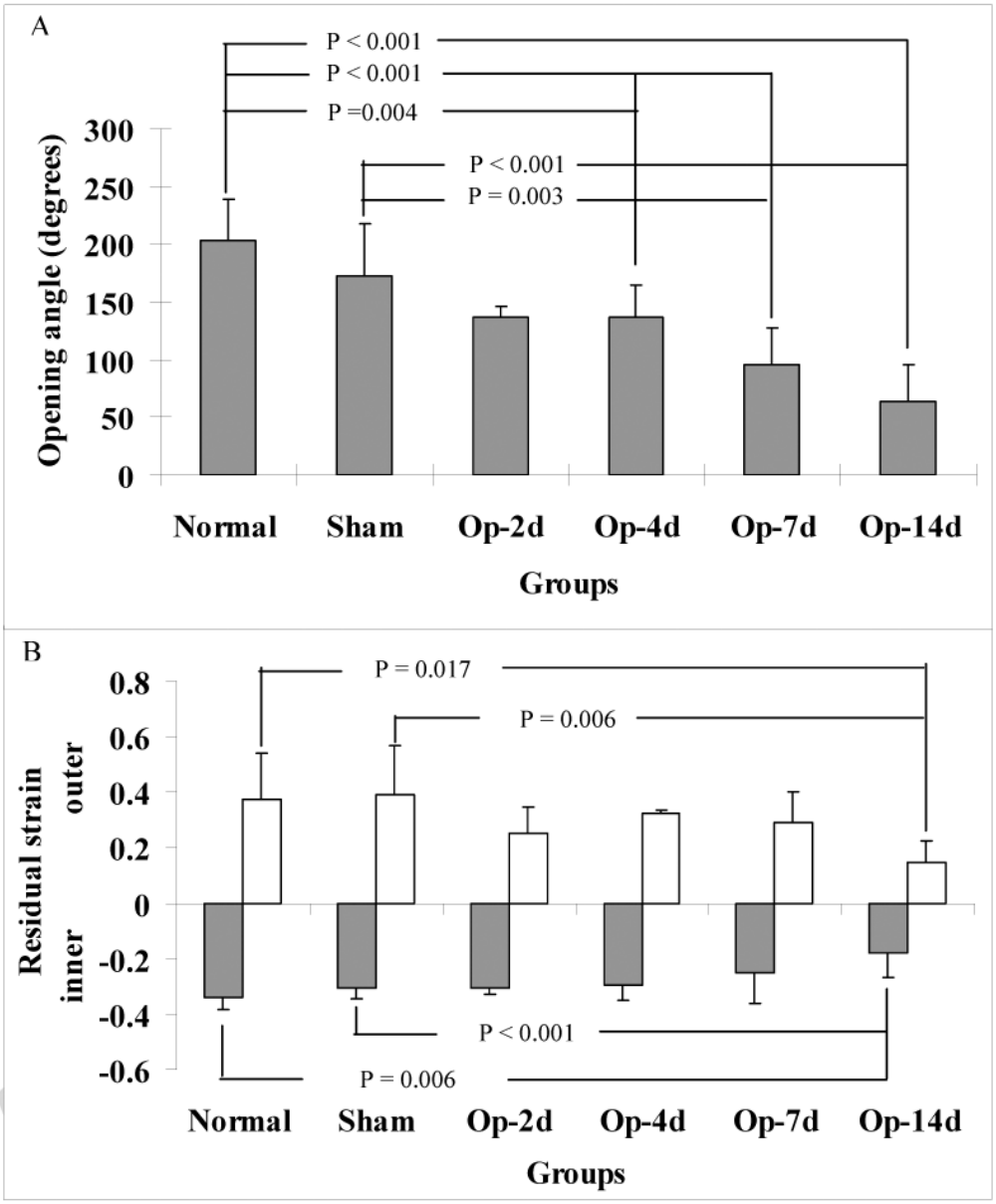

Figure 7.
The opening angles and residual strains of the intestinal segments are shown. All parameters were smaller after the obstruction when compared to those in the sham operation and normal groups.

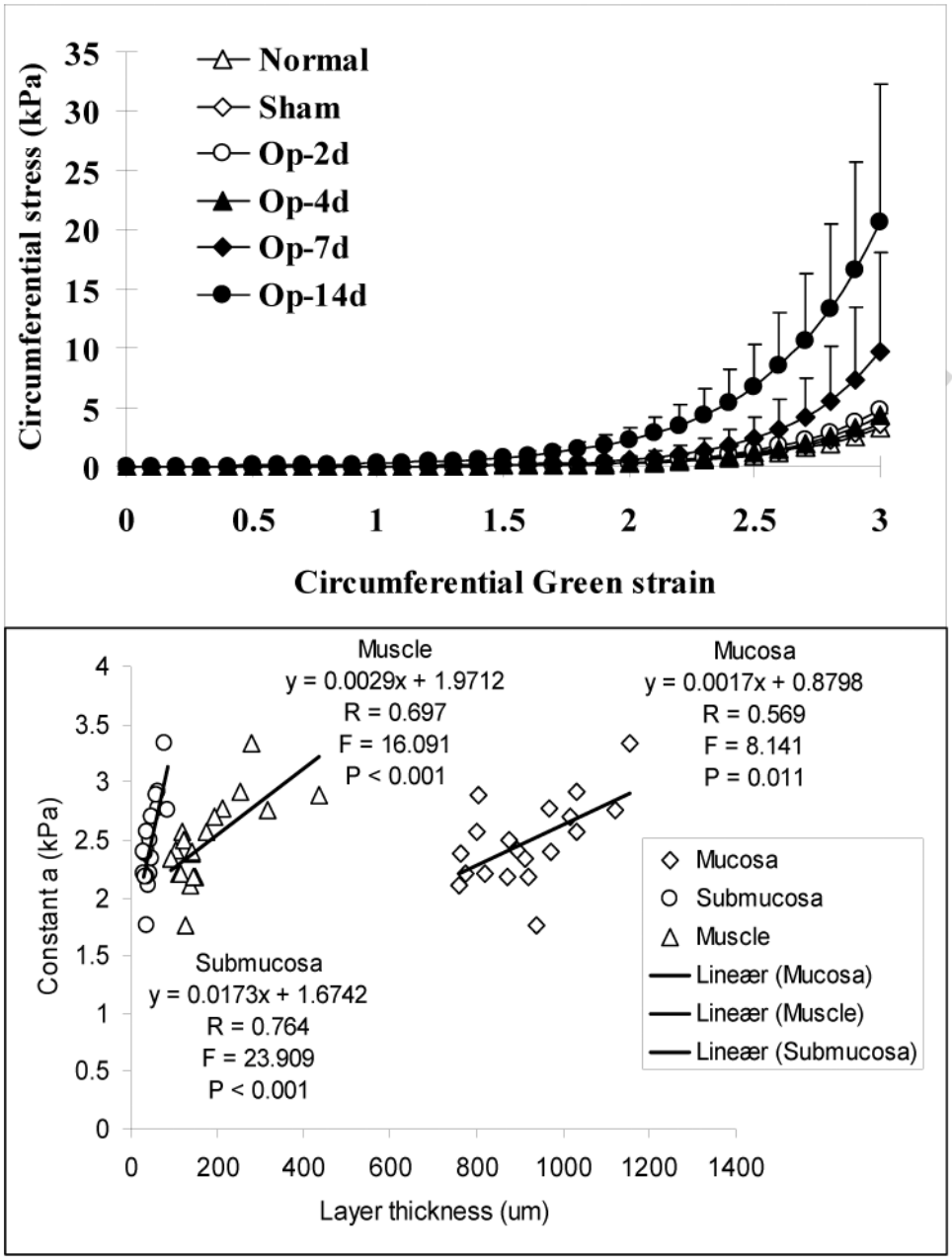

Figure 8.

Top panel: The circumferential stress-strain curves at longitudinal stretch ratio 1.1 in the groups. The stress-strain curves were shifted to the left after 7 days obstruction compared those with normal and sham control groups, indicating the intestinal wall became stiffer due to the obstruction. Bottom panel: The linear association between the constant **a** and the thickness of different layers. The strongest correlation was found between the constant **a** and the thickness of submucosa layer.

Table 1

Multiple linear regression analysis of biomechanical parameters and thickness of the layers

Biomechanical parameters	Multiple linear regression equation	intestinal layers	t value	P value
Opening angle	Opening angle = 336.079 - (0.143 * Mucosa) + (0.485 * Submucosa) - (0.534 * Muscle)	Mucosa	-1.808	0.091
		Submucosa	0.598	0.559
		Muscle	-4.382	<0.001
Inner residual strain	Inner residual strain = -0.470 + (0.0000428 * Mucosa) + (0.000270 * Submucosa) + (0.000778 * Muscle)	Mucosa	0.362	0.722
		Submucosa	0.223	0.827
		Muscle	4.274	<0.001
Outer residual strain	Outer residual strain = 0.688 - (0.000260 * Mucosa) - (0.000411 * Submucosa) - (0.000851 * Muscle)	Mucosa	-1.016	0.326
		Submucosa	-0.156	0.878
		Muscle	-2.157	0.048